Local Versus Global Equilibration near the Bosonic Mott-Insulator–Superfluid Transition

Stefan S. Natu, Kaden R. A. Hazzard, and Erich J. Mueller

Phys. Rev. Lett. **106**, 125301 — Published 23 March 2011

DOI: 10.1103/PhysRevLett.106.125301

Local versus global equilibration near the bosonic Mott-superfluid transition

Stefan S. Natu,[1,*] Kaden R. A. Hazzard,[2] and Erich J. Mueller[1]

[1] *Laboratory of Atomic and Solid State Physics, Cornell University, Ithaca, New York 14853, USA.*
[2] *JILA, NIST and Department of Physics, University of Colorado, Boulder, Colorado 80309-0440, USA*

We study the timescales for adiabaticity of trapped cold bosons subject to a time-varying lattice potential using a dynamic Gutzwiller mean-field theory. We explain apparently contradictory experimental observations by demonstrating a clear separation of timescales for local dynamics ($\sim$ ms) and global mass redistribution ($\sim$ 1s). We provide a simple explanation for the short and fast timescales, finding that while density/energy transport is dominated by low energy phonons, particle-hole excitations set the adiabaticity time for fast ramps. We show how mass transport shuts off within Mott domains, leading to a chemical potential gradient that fails to equilibrate on experimental timescales.

Introduction.— A wide range of experiments have forced us to confront questions of dynamics in strongly correlated systems. These include studies of high density nuclear matter at the Relativistic Heavy Ion Collider (RHIC) [1], transport through metal-insulator interfaces [2], and femtosecond spectroscopy [3] of quantum dots after sudden changes in gate voltages [4]. This is a conceptually rich area where computation is difficult, and where it is hard to devise experiments which are straightforward to analyze. Experiments in cold atoms are beginning to play an important role in this area – they have started providing a framework for understanding the non-equilibrium dynamics of strongly correlated materials [5–10]. In cold gas experiments, not only is the Hamiltonian known, but one can dynamically tune between weak and strong interactions, readily producing highly non-equilibrium situations that allow one to explore both linear and nonlinear responses, the reestablishment of equilibrium, and the generation of topological defects during rapid quenches [11]. The latter physics is relevant to astrophysical models of the early universe. Here we theoretically explore the timescales governing local and global transport of bosons in optical lattices, the prototypical example of strongly correlated cold atom physics.

Adding further interest to this area, initial experiments [5–7] probing the dynamics of bosons in optical lattices have found adiabaticity/relaxation timescales that differ by two orders of magnitude. The shortest of these timescales was particularly noteworthy, as it was an order of magnitude smaller than the inverse of the single particle tunneling energy, $t \sim 0.1J^{-1}$ [6]. How can the system adjust itself on a timescale which is short compared to the tunneling time? Conversely, experiments on a nearly identical system at Chicago [5], found that the global density profile didn't attain it's equilibrium value even on times $t \sim 10J^{-1}$! Here we resolve this contradiction by demonstrating a separation of timescales for global transport and local equilibration, and show that the timescale for adiabiaticity is largely set by the gap towards particle-hole excitations in the strongly correlated superfluid.

The separation of timescales for local and global equilibrium emerges in most interacting systems and materials. For example, in the air around us, local equilibrium is achieved on the collision time ($\sim$ns), but global equilibrium is limited by transport coefficients, and is relatively slow. Typically one expects the slow variables to be those that are conserved (such as density and energy density), and those which correspond to broken symmetries (such as the phase of the superfluid order parameter). Integrating out the fast variables leads to a hydrodynamic description solely in terms of the slow variables.

A practical consequence of this separation of timescales is that adiabaticity is much easier to maintain if one changes parameters in such a way that very little mass transport is necessary: a principle which is widely used in cold atom experiments. Optimizing the ramping protocol is particularly important if insulating regions develop in the cloud: the transport through these regions is highly attenuated.

Theoretical Setup.—Bosonic atoms trapped by interfering laser beams are well described by the Bose Hubbard Hamiltonian [12]

$$\mathcal{H} = -J\sum_{\langle ij\rangle}(a_i^\dagger a_j + h.c) + \sum_i \left(\frac{U}{2}n_i(n_i-1) - \mu^{\mathrm{i}} n_i\right) \quad (1)$$

where a and $a^\dagger$ are bosonic annihilation and creation operators, J is the tunneling, and U is the on-site interaction. We denote $\mu^i = \mu - V_{\mathrm{ex}}(i)$, where μ is the chemical potential and $V_{\mathrm{ex}}(i)$ is the external potential at site i. Disorder introduces a similar term in solid state Hamiltonians. The first sum is over all nearest neighbor sites in the plane. In Figure 1, we show U and J as a function of lattice depth V_R for ^{87}Rb in a $d = 680$nm lattice generated by light of wavelength $\lambda = 1360$nm, obtained from the Wannier functions [13].

We calculate dynamics using a time dependent Gutzwiller ansatz [12], which approximates the wavefunction by $\Psi = \bigotimes_i \sum_m c_m^{(i)}(t)|m\rangle_i$ where $|m\rangle_i$ is the m-particle Fock state on site i, and the coefficients $c_m^{(i)}(t)$ are generally space and time dependent. In a homogenous system [14], the excitation spectrum predicted by this

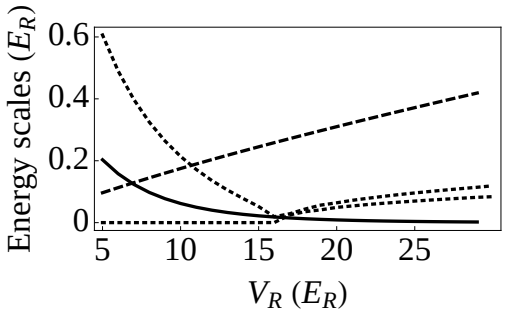

FIG. 1: **Energy scales in 2D Bose Hubbard model as a function of lattice depth [13]**: Solid: $4J$, Dashed: U, Dotted: Two lowest $k = 0$ excitations from linearizing at unity filling. Parameters: ^{87}Rb in a $d = 680$ nm lattice.In the superfluid state, the Goldstone mode has zero energy. In the Mott state, these modes represent the particle/hole excitations.

theory agrees well with other techniques [15]. Navez and Schützhold [16] have been studying systematic improvements of this method. The time-dependent Gutzwiller is sufficiently sophisticated to yield the separation of timescales which we wish to elucidate. Recent time-dependent density matrix renormalization group calculations of the 1D Bose-Hubbard model find similar results to ours [17].

This mean-field ansatz reduces Eq. 1 to a sum of single site Hamiltonians $\mathcal{H}_i = -4t(\langle\alpha_i\rangle^* a_i + \langle\alpha_i\rangle a_i^\dagger) + 4t|\langle\alpha_i\rangle|^2 + \frac{U}{2}n_i(n_i-1) - [\mu - V(i)]n_i$ at each site i. Truncating the basis at each site to a maximum M particles, $\mathcal{H}_i$ is an $(M+1)\times(M+1)$ matrix at each site, and depends on the other sites only through $\langle\alpha_i\rangle = (1/4)\sum_{\langle j\rangle}\langle a_j\rangle$, where $\langle a_j\rangle = \sum_m \sqrt{m+1}c_{m+1}^{(j)}c_m^{(j)}$, and the sum over j includes all four nearest neighbor sites.

Schrödinger's equation $i\partial_t\psi = \mathcal{H}\psi$ for Ψ yields a set of differential equations for the c_m^i:

$$i\partial_t c_m^i(t) = -4J(t)(\langle\alpha_i\rangle^*\sqrt{m+1}c_{m+1}^i + \langle\alpha_i\rangle\sqrt{m}c_{m-1}^i) + \left(\frac{U(t)}{2}m(m-1) - \mu^i m + 4J(t)|\langle\alpha_i\rangle|^2\right)c_m^i \quad (2)$$

The tunnelings ($J(t)$) and on-site interactions ($U(t)$) are dynamically tuned by changing the lattice depth in time. We study population dynamics across the superfluid-insulator transition by ramping the lattice linearly in time using the protocol $V(t) = V_\mathrm{i} + (V_\mathrm{f} - V_\mathrm{i})(t/\tau_\mathrm{r})$, where V_i and V_f are the initial and final lattice depths, and τ_r is the ramp time. We consider a time independent radially symmetric harmonic trap, $V_\mathrm{ex} = \frac{1}{2}m\omega^2(x^2+y^2)$.

We approximate the ground state by finding the stationary solution to Eq. (2), $c_m^i(t) = e^{-i\epsilon t}c_m^i$, where ϵ can be identified with the energy per site. We use an iterative algorithm, starting with a trial α_i, then find c_m^i by solving the eigenvalue problem in Eq. (2). We calculate a new α_i and repeat until the subsequent change in α_i is sufficiently small. To calculate time dynamics, we use sequential site updates [18] in order to conserve total particle number and energy (for time-independent Hamiltonians).

The resulting dynamics describe the behavior of a single quantum state, rather than a density matrix. Nevertheless, the equations governing the time dependent Gutzwiller ansatz are highly nonlinear and contain a large number of degrees of freedom. This structure is rich enough that under appropriate conditions time dynamics leads to thermalization, with (on average) energy equally distributed among all modes.

Results.—We consider several different scenarios in order to fully explore the response of this system to a lattice ramp. We start by analyzing a homogeneous system: this investigation yields the timescale for maintaining local equilibration. This timescale sets the fundamental limit for how fast equilibration can take place in the absence of global mass transport. Similar to the Harvard experiments [6], we find that local equilibrium can be maintained even under surprisingly rapid quenches through the superfluid-Mott boundary.

Next we explore the requirements for maintaining global equilibrium. We show that equilibration times are much longer in systems requiring large amounts of particle transport. This situation is exacerbated by the presence of large Mott domains.

We conclude by showing that rapid *global* equilibration can be achieved if the trap parameters are chosen in a way as to minimize transport between intervening Mott shells. Our results in this section are consistent with the Münich experiments [7].

Local equilibration.—In an isolated homogeneous system, ramping the depth of an optical lattice does not lead to bulk mass transport. Instead, all of the temporal dynamics simply involve the evolution of number fluctuations and correlations. Thus equilibration is governed by local physics and Eq. (2) reduces to the single site problem. We numerically integrate this nonlinear set of ordinary differential equations, taking J and U functions of time, corresponding to a linear ramp of the lattice from depth V_i to V_f. We vary V_i, V_f, and the ramp time τ_r. We take all parameters to correspond to ^{87}Rb atoms, and take $n = 1$ particles per site.

At unity filling, near the Mott transition, we truncate the basis to at most 2 particles per site. In this truncated basis, the probability of having a single particle per site $P(1)$ is identical to the probability of having an odd number of particles per site, which is the experimental observable in the Harvard experiments [6].

Both the gapped $q = 0$ single-particle excitations (see Fig.1 and Ref.[15]), and the continuum of two-phonon excitations contribute to the non-adiabatic evolution. All of these modes are captured in a time-dependent Gutzwiller framework [14]. One expects that the number of excitations goes to zero as the ramp rate vanishes. When gapped excitations of energy Δ dominate the dissipation, then the condition for adiabaticity is $\frac{1}{\Delta^2}d\Delta/dt \ll 1$ [19].

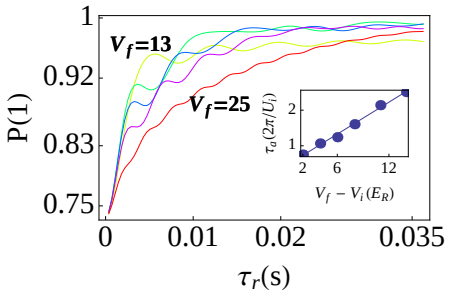

FIG. 2: (Color Online) **Population dynamics at unity density** $n = 1$ (Top): Probability of having one particle per site at the end of a lattice ramp from $V_i/E_R = 11$ lattice to (top to bottom) $V_f/E_R = 13$(yellow), 15(green), 17(blue), 19(purple) and 25(red) after different lattice ramp times $\tau_r = 0.1/U_i \sim 0.3$ms to $10/U_i$. Inset: Characteristic timescale τ_a extracted from exponential fits to main figure. Fig.(3) of [6].

In Fig. 2 we show that the timescale for local equilibration is very short. Starting with a superfluid at $V_i = 11E_R$, we ramp up to different lattice depths. We plot the time evolution of the probability that a single particle sits at a given site as we vary the the ramp time τ_r from $0.1\hbar/U_i$ to $10\hbar/U_i$, where $U_i = \hbar/3$ms. This procedure is identical to that used in the Harvard experiments [6]. Fitting these curves to simple exponentials yields a characteristic timescale τ_a, which, as we show in the inset, is comparable to U_i^{-1} – a typical gap to particle-hole excitations (Fig. 1). We conclude that these particle-hole excitations are dominating the non-adiabatic processes.

Inhomogeneous dynamics.—We now consider an inhomogenous system by imposing a harmonic external potential on top of the lattice. The protocol for lattice ramps is same as before, starting with a superfluid at 11 recoil lattice depth. The central chemical potential is chosen such that the central density is close to unity, justifying the truncated basis ($M = 2$) used here. Throughout we define time in units of $2\pi/U_i$ where U_i is the on-site interaction at $V_i = 11E_R$ equal to $\sim 2\pi \times 300$Hz. We use a trapping frequency of $\omega = 25$Hz.

In Fig. 3 we plot the density profile after a lattice ramp from $V_i = 11E_R$ to $V_f = 16E_R$ in a time $t = 120 \times 2\pi/U_i$ for a system 30×30 sites containing 500 particles. As shown already, this ramp is sufficiently slow to be locally adiabatic. The parameters are chosen such that at later times a large Mott region separates the central superfluid from the superfluid at the edge.

We find that after this ramp the density profile of the final state (dashed line) is very different from the equilibrium state at V_f(dotted red), implying a relaxation time much longer the ramp time of 400ms. Indeed, further simulations show that it is longer than the experimental timescale of seconds. In the remainder of this paper we describe the cause of the slow equilibration, and conduct a number of additional simulations to illustrate how equilbration times depend on the various experimental parameters.

The major bottleneck for equilibration in Fig. 3 is mass transport across the Mott region [20]. To illustrate the spatial location of the Mott insulator, in Fig. 3(b) we plot the coherences $\mathcal{C}_i \equiv -\langle a_i \rangle \sum_j \langle a_j^* \rangle$ as a function of time, where i, j denote nearest neighbor pairs. Mott regions ($\mathcal{C} = 0$) show up as dark regions in the density plot. The Mott plateau widens over time, isolating the central superfluid. The peak atomic density in the initial lattice exceeds that of the equilibrium state at the final lattice depth. However the Mott region prevents mass flow from the center to the edge.

Integrating out the fast variables will lead to hydrodynamic equations of the form $\frac{\partial}{\partial t} n + \nabla \cdot \mathbf{j} = 0$ and $\frac{\partial}{\partial t} \mathbf{j} = -(n/m_{\rm eff}) \left[(1/n) \nabla P + \nabla V \right] + \Gamma_j$ where $\mathbf{j} = n\mathbf{v}$ is the particle current, P is the pressure, V is the external potential, and Γ_j encodes viscous forces and terms which are higher order in the velocity and gradients of the thermodynamic functions. This equation defines the effective mass $m_{\rm eff}$, which can be extracted from the speed of sound c and compressibility κ by $m_{\rm eff} = 1/\kappa c^2$. In particular $m_{\rm eff}$ diverges in Mott regions, where transport becomes diffusive. One naturally is lead to a circumstance where Mott domains break the cloud is into discrete superfluid regimes, each of which has independent chemical potentials and temperatures.

This structure is elucidated in Fig.3 where we use the zero temperature equation of state to plot $\mu[n(r)] + V(r)$ as a function of space. In equilibrium, local density approximation predicts $\mu[n(r)] + V(r) = \mu_0$, a constant. One sees that $\nabla \left[\mu + V \right] = (1/n)(\nabla P - S \nabla T) + \nabla V = 0$ in each superfluid region, but that there is a gradient in $\mu + V$ as one crosses the Mott domain. This clearly shows that while the superfluid regions have equilibrated amongst themselves, they are not in equilibrium with each other.

A similarly long lived metastable configuration is believed to occur at the superfluid-normal interface of a population imbalanced Fermi gas, where regions of polarized normal gas in local chemical equilibrium, are separated by an intervening superfluid region, with a spin gap, that acts as a barrier to transport [21, 22].

Fast equilibration without transport.—Now we show that equilibration times can be dramatically reduced when parameters are chosen such that no bulk transport across Mott regions is required. The parameters are chosen to mimic the systems considered by Sherson *et al.* [7], which attained *global* equilibrium on timescales comparable to 100ms. Figure 4 shows the time-evolution of an initial state at $V_i = 11$ at $N = 800$ in 2.5Hz trap, and a central chemical potential of $\mu = 1.4U$. We find that after an evolution of $\tau_r = 25 \times 2\pi/U_i$, the final profile (dashed) is close to the equilibrium $T = 0$ Gutzwiller prediction (dotted).

Despite the fact that the $n = 1$ Mott region is of similar size as Fig.3, we find faster equilibration times in this

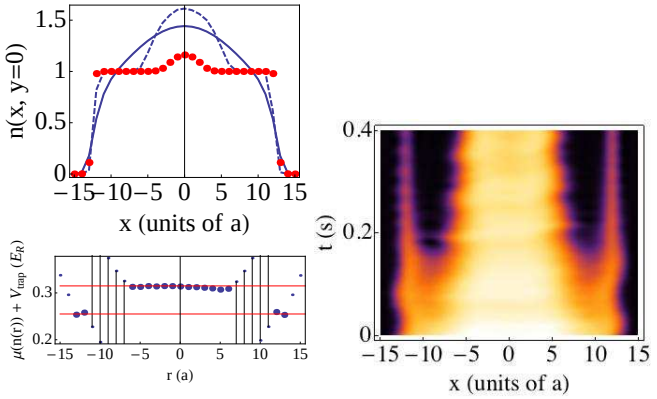

FIG. 3: (Color Online) **Slow transport across Mott region** (Top-Left) Evolution of an initial (solid) superfluid state at $V_{\rm i} = 11E_R$ and $N = 500$ in a 25Hz radial trapping potential. Final density profile (dashed) after a ramp $\tau_r = 120 \times 2\pi/U_{\rm i} \sim 400$ ms, is very different from the equilibrium state (dotted) at $V_{\rm f} = 16E_R$. (Right) Density plot of the time evolution of the coherences ($\mathcal{C}_i \equiv -\langle a_i\rangle \sum_j \langle a_j^*\rangle$) features a growing Mott region which cuts off transport between the superfluid regions in the center and the edge, leading to a non-equilibrium final state at late times. Brighter colors correspond to larger $\mathcal{C}$. (Bottom-Left): A chemical potential gradient is established between the superfluid regions after dynamics ($t = 400$ms, dots). Within the Mott domain, μ is not a unique function of n, and vertical lines illustrate the range of values of the ordinate. In the initial state $\mu + V(r) = \mu_0$ is a constant. At the wings there are no particles and $\mu + V(r) \sim V(r)$. The fact that $\mu + V(r)$ is roughly constant in the superfluid regions confirms that they are in local equilibrium.

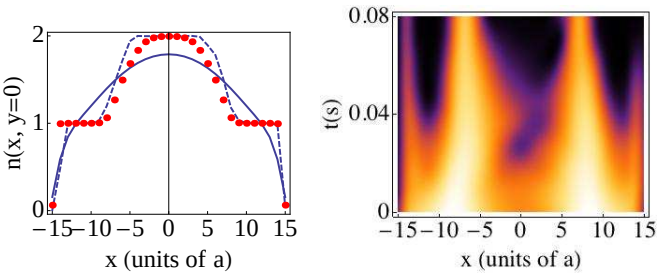

FIG. 4: (Color Online) **Fast equilibration in absence of transport**(Left): Evolution of an initial superfluid state for $V_{\rm i} = 11E_R$ and $N = 800$ (solid) in a 25Hz radial trapping potential in a linear ramp with $\tau_{\rm r} = 25 \times 2\pi/U_{\rm i} = 80$ms. The dotted profile is the $T = 0$ equilibrium Gutzwiller profile at $V_0 = 16E_R$ for the same parameters. The final density profile (dashed) agrees with the $T = 0$ equilibrium Gutzwiller profile. (Right): Time evolution of the spatial coherence distribution, showing the formation of an $n = 1$ and $n = 2$ Mott plateaus. Lighter colors imply larger coherences. Cf. Fig.(2) in [7].

system. The difference is that here parameters are chosen such that the total number of particles in the center is the same in the initial and final states. Thus no transport is needed across the Mott region.

Summary.—Motivated by experiments, we have demonstrated a separation of timescales for local and global equilibration for trapped bosons in optical lattices. We also showed that the presence of a wide Mott region can inhibit transport, producing isolated superfluid regions which are in local equilibrium, but which have differing chemical potentials. The timescale for maintaining local equilibrium is extremely short, being primarily governed by gapped single-particle excitations.

Acknowledgements.—This work was supported in part by a grant from the Army Research office with funding from the DARPA OLE Program. SN thanks S. K. Baur for insightful discussions. KRAH thanks Ana Maria Rey for useful discussions and support.

* Electronic address: ssn8@cornell.edu

[1] N Demir and S. A. Bass, Phys. Rev. Lett. **102** 172302 (2009).
[2] S. V. Kravchenko, *et al.* Phys. Rev. B **51** 7038 (1995).
[3] P.C. Becker, *et al.*, Phys. Rev. Lett **61** 1647 (1988).
[4] S. Cronenwett, Tjerk H. Oosterkamp and L. P. Kouwenhoven, Science, **281** 5736 (1998).
[5] C. Hung *et al.* Phys. Rev. Lett. **104**, 160403 (2010).
[6] W. S. Bakr, *et al.* Science **329**, 547–550 (2010).
[7] J. F. Sherson, *et al.* Nature **467**, 68(2010).
[8] T. Kinoshita, T. Wenger, and D. S. Weiss, Nature **440**, 900 (2006).
[9] L Hackermüller, *et al.*, Science, **327** 5973 (2010).
[10] C. Cao, *et al.*, Science, **331** 58 (2010).
[11] M. Rigol, V. Dunjko, and M. Olshanii, Nature **452**, 854 (2008); K. Sengupta, S. Powell, and S. Sachdev, Phys. Rev. A **69**, 053616 (2004); W. H. Zurek, U. Dorner, and P. Zoller, Phys. Rev. Lett. **95**, 105701 (2005); Schutzhold *et al.* ibid. **97** 200601 (2006).
[12] M. P. A. Fisher *et al.* Phys. Rev. B **40**, 546–570 (1989).
[13] D. Jaksch *et al.* Phys. Rev. Lett. **81**, 3108–3111 (1998).
[14] K. V. Krutitsky and P. Navez, arxiv:1004.2121 (2010),
[15] C. Menotti and N. Trivedi, Phys. Rev. B **77**, 235120 (2008).
[16] P. Navez and R. Schützhold, arxiv:1008.1548 (2010),
[17] J-S Bernier, G. Roux, and C. Kollath, arxiv:1010.5251 (2010).
[18] J. Wernsdorfer, M. Snoek, and W. Hofstetter, Phys. Rev. A **81**, 043620 (2010).
[19] L. D. Landau and L. M. Lifshitz, *Quantum Mechanics* (Butterworth-Heinemann, 1981).
[20] S. Vishveshwara and C. Lannert, Phys. Rev. A **78**, 053620 (2008).
[21] G. B. Partridge, *et al.*, Phys. Rev. Lett. **97** 190407 (2006).
[22] M. M. Parish and D. A. Huse Phys. Rev. A **80** 063605 (2009).